

TOPICAL REVIEW

Micromixers—a review

To cite this article: Nam-Trung Nguyen and Zhigang Wu 2005 *J. Micromech. Microeng.* **15** R1

View the [article online](#) for updates and enhancements.

You may also like

- [Micromixing optimization of non-newtonian fluids with heterogeneous zeta potential](#)
Anshul Kumar Bansal, Gajendra Kumar Nhaichaniya, Mayank Bhardwaj et al.
- [A novel application of dielectric stack actuators: a pumping micromixer](#)
Susana Solano-Arana, Florian Klug, Holger Mößinger et al.
- [Electrochemical detection of baicalein based on a three-dimensional micromixer](#)
Jie Liang, Jianfeng Yu, Yang Cheng et al.



PRIMETM
PACIFIC RIM MEETING
ON ELECTROCHEMICAL
AND SOLID STATE SCIENCE
HONOLULU, HI
October 6-11, 2024

Joint International Meeting of
The Electrochemical Society of Japan (ECSJ)
The Korean Electrochemical Society (KECS)
The Electrochemical Society (ECS)

Early Registration Deadline:
September 3, 2024

**MAKE YOUR PLANS
NOW!**

TOPICAL REVIEW

Micromixers—a review

Nam-Trung Nguyen and Zhigang Wu

School of Mechanical and Production Engineering, Nanyang Technological University,
50 Nanyang Avenue, Singapore 639798, Singapore

E-mail: mntnguyen@ntu.edu.sg

Received 15 July 2004, in final form 11 October 2004

Published 8 December 2004

Online at stacks.iop.org/JMM/15/R1**Abstract**

This review reports the progress on the recent development of micromixers. The review first presents the different micromixer types and designs. Micromixers in this review are categorized as passive micromixers and active micromixers. Due to the simple fabrication technology and the easy implementation in a complex microfluidic system, passive micromixers will be the focus of this review. Next, the review discusses the operation points of the micromixers based on characteristic dimensionless numbers such as Reynolds number Re , Peclet number Pe , and in dynamic cases the Strouhal number St . The fabrication technologies for different mixer types are also analysed. Quantification techniques for evaluation of the performance of micromixers are discussed. Finally, the review addresses typical applications of micromixers.

Nomenclature

ν	kinematic viscosity ($\text{m}^2 \text{s}^{-1}$)
θ	angle (rad)
c	concentration of a species (kg m^{-3})
c^*	dimensionless concentration
D	diffusion coefficient ($\text{m}^2 \text{s}^{-1}$)
D_h	hydraulic diameter (m)
f	disturbance frequency (Hz)
H	channel height (m)
K_n	modified Bessel function of the second kind n -order
L	mixing path (m)
m	number of serial mixing stages
n	number of laminae
Q_1, Q_2	flow rates ($\text{m}^3 \text{s}^{-1}$)
R	radius of injection nozzle (m)
r	mixing ratio
r^*	dimensionless radius
U	average flow velocity (m s^{-1})
W	channel width (m)
Pe	Peclet number
Re	Reynolds number
St	Strouhal number

1. Introduction

Miniaturization is the recent trend in analytical chemistry and life sciences. In the past two decades, miniaturization of fluid handling and fluid analysis has been emerging in the interdisciplinary research field of microfluidics. Microfluidic applications cover micro arrays, DNA sequencing, sample preparation and analysis, cell separation and detection, as well as environmental monitoring. The use of microfluidics in these applications attracts interest from both industry and academia, because of its potentials and advantages: small amounts of sample and reagent, less time consumption, lower cost and high throughput. The number of archival journal papers on microfluidics has been increasing almost exponentially. A few books dedicated to microfluidics are also recently available [1–3].

Besides the micropump, the micromixer is another important component in a microfluidic system. Nguyen *et al* [4], and recently Laser and Santiago [5] as well as Woias [6], dedicated their reviews to micropumps. In contrast, no extensive review on micromixers exists. Kakuta *et al* gave an early review on micromixers [7]. A section in the book of Nguyen and Wereley [1] was dedicated to only a few types of micromixers. Some general review papers on micro total analysis systems (microTAS) by Reyes *et al* [8], Auroux *et al* [9], Vilkner *et al* [10] and Erbacher *et al* [11] also dealt briefly

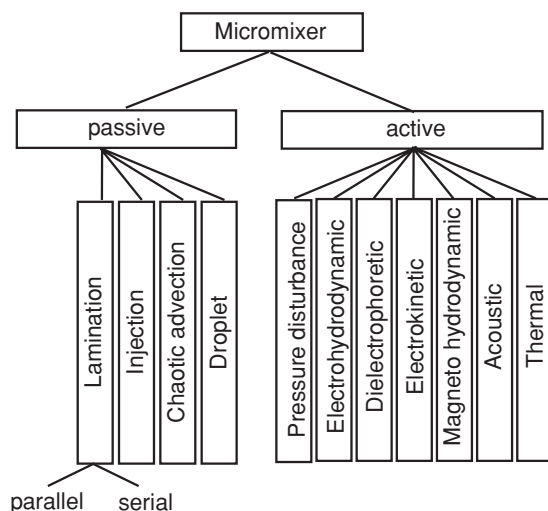


Figure 1. Classification scheme for micromixers.

with micromixers. In the past, the importance of micromixers was not well recognized and only a few research groups were focused on this area. Recently, a number of new micromixers have been widely published in research journals. In fact, most of the works reviewed in this paper were published in the past 3 years. The recent emerge of micromixers deserves a systematic review, which could benefit the microfluidics community.

Rapid mixing is essential in many of the microfluidic systems used in biochemistry analysis, drug delivery and sequencing or synthesis of nucleic acids. Biological processes such as cell activation, enzyme reactions and protein folding often involve reactions that require mixing of reactants for initiation. Mixing is also necessary in lab-on-a-chip (LOC) platforms for complex chemical reactions. Micromixers can be integrated in a microfluidic system or work as stand-alone devices. Furthermore, the investigation of micromixers is fundamental for understanding transport phenomena on the microscale.

Previously, the fabrication of micromixers was based on technologies of micro electromechanical systems (MEMS) [12]. The basic substrate materials were silicon and glass. Recently, arising from the need for low cost and biocompatibility, polymers have been extensively used for making micromixers. A number of polymeric fabrication techniques are readily available. Polymeric bulk micromachining such as hot embossing, injection molding, casting and laser ablation, realized structures in a polymer substrate, while polymeric surface micromachining creates movable polymeric microstructures using a sacrificial layer.

In general, micromixers can be categorized as passive micromixers and active micromixers (figure 1). Passive micromixers do not require external energy, the mixing process relies entirely on diffusion or chaotic advection. Passive mixers can be further categorized by the arrangement of the mixed phases: parallel lamination, serial lamination, injection, chaotic advection and droplet. Active micromixers use the disturbance generated by an external field for the mixing process. Thus, active mixers can be categorized by the types of external disturbance effects such as pressure, temperature,

electrohydrodynamics, dielectrophoretics, electrokinetics, magnetohydrodynamics and acoustics. With external fields and the corresponding integrated components, the structures of active micromixers are often complicated and require complex fabrication processes. Furthermore, external power sources are needed for the operation of active micromixers. Thus, the integration of active mixers in a microfluidic system is both challenging and expensive. In contrast, passive micromixers do not require external actuators except those for fluid delivery. The often simple passive structures are robust, stable in operation and easily integrated in a more complex system. In this review, more attention is given to passive micromixers.

For general references on mixing, some excellent books and review papers are available. Einstein's theory on the thermal motion of molecules [13] is the foundation for diffusion theory. For mixing on the macroscale readers can refer to the review of Ottino [14]. On the macroscale the common mixing methods are the generation of turbulence [15] and chaotic advection [16, 17]. In a turbulent flow, fluid motions vary irregularly so that quantities such as velocity and pressure show a random variation in time and space. The random movement quickly disperses the mixed components. Chaotic advection can be generated by stirring the flow, which is very effective for small Reynolds numbers. The concepts of splitting, stretching, folding and breaking up are critical for the mixing quality. For more elaborate sources on diffusion theory readers may refer to the book of Cussler [18] or that of Cunningham and William [19]. Another text book about all transport phenomena is written by Bird *et al* [20], which is very useful for understanding the flow behaviour in micromixers.

This review first considers the various micromixer types. The operation conditions of the reviewed micromixers are then discussed. Attention is paid to a number of operating parameters such as the Reynolds number Re , the Peclet number Pe and the Strohal number St . The Reynolds number:

$$Re = \frac{UD_h}{\nu} \quad (1)$$

represents the ratio between momentum and viscous friction. A high Reynolds number above a critical value (around 2300 on the macroscale) indicates a turbulent flow. In most cases of microfluidics, a low Reynolds number and a laminar flow can be expected. The Peclet number:

$$Pe = \frac{UL}{D} \quad (2)$$

represents the ratio between the mass transport due to convection and that of diffusion. Convection is domina at higher Peclet numbers. The Strohal number:

$$St = \frac{fD_h}{U} \quad (3)$$

represents the ratio between the residence time of a species and the time period of its disturbance in an active micromixer.

2. Passive micromixers

Because of its simple concept, the passive mixer was one of the first microfluidic devices reported. Due to the dominating laminar flow on the microscale, mixing in passive micromixers relies mainly on molecular diffusion and chaotic advection.

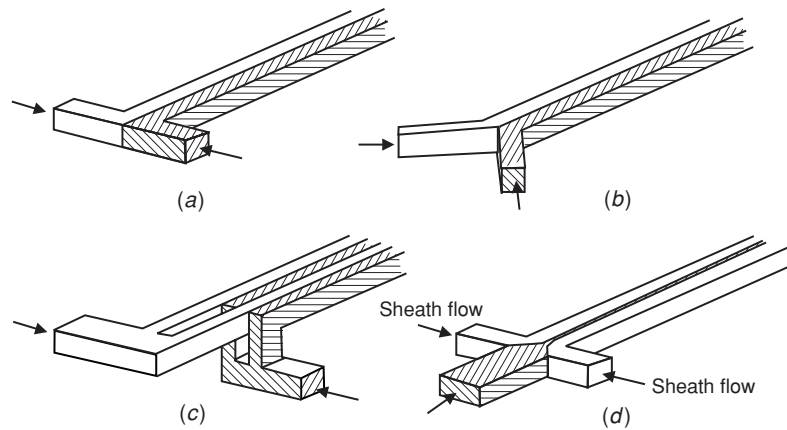


Figure 2. Parallel lamination micromixer: (a) the basic T-mixer and (b) Y-mixer, (c) the concept of parallel lamination and (d) the concept of hydraulic focusing.

Increasing the contact surface between the different fluids and decreasing the diffusion path between them could improve molecular diffusion. Chaotic advection can be realized by manipulating the laminar flow in microchannels. The resulting flow pattern shortens the diffusion path and thus improves mixing.

2.1. Parallel lamination micromixers

As mentioned above, fast mixing can be achieved by decreasing the mixing path and increasing the contact surface between the two phases. Parallel lamination splits the inlet streams into n substreams, then join them into one stream as laminae. The basic design is a long microchannel with two inlets ($n = 2$) to its geometry; these designs are often called the T-mixer or the Y-mixer [21–23] (figures 2(a) and (b)). For a flat mixing channel ($W \gg H$), the concentration distribution in the mixing channel can be derived analytically, (figure 3(a)). Assuming the same viscosity in each stream, and thus a uniform flow velocity U , the dimensionless concentration distribution $c^* = c/C_0$ in the microchannel for an arbitrary mixing ratio between a solute ($c = C_0$) and a solvent ($c = 0$) of $r : (1 - r)$ is

$$c^*(x^*, y^*) = r + \frac{2}{\pi} \sum_{n=1}^{\infty} \frac{\sin n r \pi}{n} \cos(n \pi y^*) \times \exp\left(-\frac{2n^2 \pi^2}{Pe + \sqrt{Pe^2 + 4n^2 \pi^2}} x^*\right) \quad n = 1, 2, 3, \dots \quad (4)$$

where $x^* = x/W$, $y^* = y/W$ are dimensionless coordinates, $Pe = UW/D$ is the Peclet number, W is the channel width and D is the diffusion coefficient (figure 3(b)). The solution (4) (figure 3(c)) can be extended for the case of parallel lamination of multiple streams (figure 3(d)). The inlet streams of a T-mixer can be twisted and laminated as two thin liquid sheets to reduce the mixing path [24]. As a basic design, the T-mixer is ideal for investigations of basic transport phenomena on the microscale, such as scaling law, the butterfly effect [21, 23] and other nonlinear effects [25].

Since the basic T-mixer entirely depends on molecular diffusion, a long mixing channel is needed. Besides the above-mentioned concept of lamination of multiple streams, mixing at extremely high Reynolds numbers could also result in a short mixing length [26, 27]. A chaotic flow is expected at these high Reynolds numbers. The induced vortices significantly enhance the mixing efficiency. In the work of Yi and Bau [26], a Y-mixer made of co-fired ceramic tapes with a 90° bend can generate vortices at Reynolds numbers above 10. At Reynolds numbers higher than 30, mixing is achieved right after the bend. Wong *et al* [27] reported a T-mixer fabricated from glass/silicon. This mixer utilizes Reynolds numbers up to 500, where flow velocity can be as high as 7.60 m s^{-1} at a driven pressure of up to 7 bar. Under extremely high Reynolds numbers ($Re = 245$, 45 m s^{-1}) a fluid flow can also generate high shear to drive very fast circulation in a diamond-shaped cavity close to a straight microchannel [28]. Fast vortices are generated to enhance mixing with multiple inlet streams focused in a circular chamber as reported by Böhm *et al* [29]. In these micromixers, the high velocities on the order of 1 m s^{-1} (7.6 m s^{-1} in [27]), 10 m s^{-1} [29] or even higher (up to 45 m s^{-1} in [28]) require high supply pressures. The high pressure (1.0 bar to 5.5 bar in [27] and 15 bar in [29]) can be a serious challenge for bonding and interconnection technologies. The basic T-design can be improved by roughening the channel wall [30] or throttling the channel entrance [31]. At high Reynolds numbers the basic T-mixer can be further modified with obstacles, which generate vortices and chaotic advection. These types are dealt with later in section 2.4.1.

A simple method to reduce the mixing path is to make a narrow mixing channel [32], realizing parallel lamination with multiple streams [33–35] (figure 2(c)) or with 3D interdigitated mixing streams [36]. Bessoth *et al* reported a parallel lamination mixer with 32 streams that can achieve full mixing in 15 ms [37]. This mixer type was successfully used in a practical analysis [38]. The flow in micromixers based on parallel lamination is usually driven by pressure, but can also be generated by electro-osmosis as reported by Fluri *et al* [39], Hadd *et al* [40] and Jacobson *et al* [41].

Another concept of reducing mixing path for parallel lamination micromixers is hydrodynamic focusing [42]. The

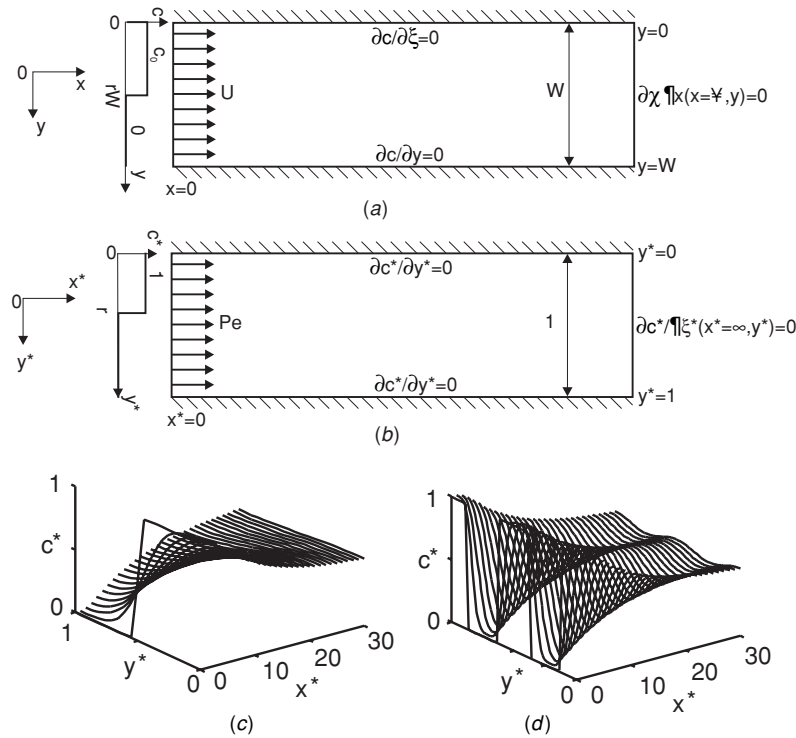


Figure 3. Concentration distribution in a parallel lamination micromixer: (a) the 2D model, (b) the dimensionless 2D model, (c) the result for the basic T-mixer ($n = 1$, $r = 0.5$) and (d) the result with multiple streams ($n = 5$, $r = 0.5$).

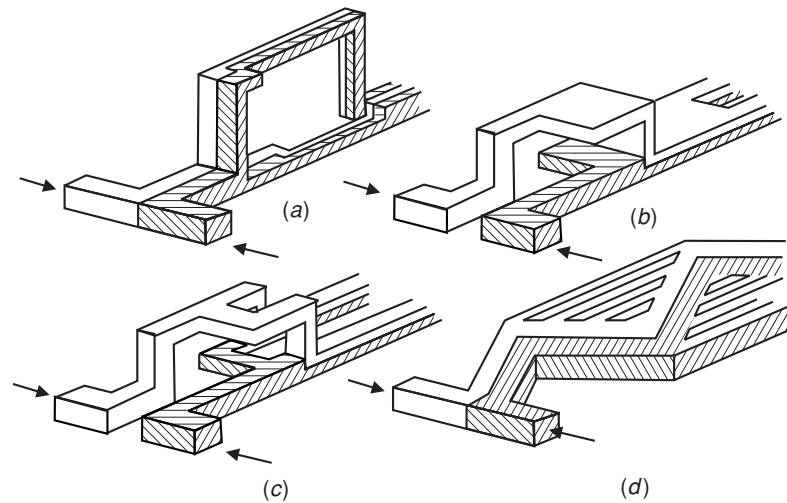


Figure 4. Serial lamination mixer: (a) join-split-join, (b) split-join [45], (c) split-split-join [48] and (d) multiple intersecting microchannels [49].

basic design for hydrodynamic focusing is a long microchannel with three inlets. The middle inlet is for the sample flow, while the solvent streams join through the other two inlets and work as the sheath flows (figure 2(d)). Hydrodynamic focusing reduces the stream width, and consequently the mixing path. Knight *et al* [42] reported a prototype that has a mixing channel of $10 \mu\text{m} \times 10 \mu\text{m}$ cross section. The sample fluid can be focused to a narrow width by adjusting the pressure ratio between the sample flow and the sheath flow. In the reported experiments, the mixing time can be reduced to a

few microseconds [43]. Walker *et al* reported the use of hydrodynamic focusing and mixing for cell infection [44]. Table 1 compares the above parallel micromixers.

2.2. Serial lamination micromixers

Similar to parallel lamination micromixers, serial lamination micromixers also enhance mixing through splitting and later joining the streams (figure 4(a)) [45–48]. The inlet streams are first joined horizontally and then in the next stage vertically.

Table 1. Parallel lamination micromixers.

Reference	First author	Year	Type	Channel width (μm)	Channel height (μm)	Typical velocity (mm s^{-1})	Re	Pe	Materials
[21, 22]	Kamholz	1999	T-mixer	550	25	6	0.3	725	Silicon–glass
[23]	Ismagilov	2000	Y-mixer	90	90	7	0.4	240	PDMS–glass
[24]	Hinsmann	2001	Y-mixer	1000	20	83	1.7	830	CaF ₂ –SU8–metal–glass
[25]	Wu	2004	Y-mixer	900	50	0.27	0.02	150	PMMA
[26]	Yi	2003	Y-mixer	200	200	50–200	80	80 000	Ceramic
[27]	Wong	2004	T-mixer	100	50	7000	500	70 000	Silicon–glass
[29]	Böhm	2001	Vortex	20	200	10000	200	200 000	Silicon–glass
[30]	Wong	2003	Cross-shaped	30	40	5000–10 000	170–340	150 000	Ceramic
[31]	Gobby	2001	T-mixer	500	300	0.3	0.1	150	n/a
[32]	Veenstra	1999	T-mixer	100	200	0.17	0.023	170	Silicon–glass
[35]	Koch	1999	Parallel lamination	85	5	0.7	0.0035	60	Silicon–glass
[37]	Bessoth	1999	Parallel lamination	20	50	1.5	0.07	60	Glass
[40]	Hadd	1997	T-mixer	35	9	1	0.014	35	Glass
[42]	Knight	1998	Focusing	10	10	50	0.5	500	Silicon–PDMS–glass
[44]	Walker	2004	Focusing	200–1000	150	1	0.15	200	PDMS–glass

n/a: not applicable.

After m splitting and joining stages 2^m liquid layers can be laminated. The process leads to a 4^{m-1} times improvement in mixing time. The mixers (figure 4(b)) reported by Branebjerg *et al* [45], Schwesinger *et al* [46] and Gray *et al* [47] were fabricated in silicon using the wet etching in KOH or deep reactive ion etching (DRIE) technique. Recently, the same approach was employed by Munson and Yager utilizing the lamination of multiple polymer layers [48] (figure 4(c)).

The concept of the serial lamination micromixer can also be applied to electrokinetic flows as reported by He *et al* [49] (figure 4(d)). Using electro-osmosis flows between the multiple intersecting microchannels, mixing is clearly enhanced. A similar design for a pressure-driven flow was reported by Melin *et al* [50]. However, this design only works for a plug of the two mixed liquids. Table 2 lists the typical parameters of serial lamination micromixers.

2.3. Injection micromixers

The concept of the injection mixer [51–55] is similar to the parallel lamination mixer. Instead of splitting both inlet flows, this mixer type only splits the solute flow into many streams and injects them into the solvent flow. On top of one stream is an array of nozzles, which create a number of microplumes of the solute. These plumes increase the contact surface and decrease the mixing path. Mixing efficiency can be improved significantly.

Figure 5(a) describes the two-dimensional model of the microplume from a single circular nozzle of an injection mixer. The mixing chamber has a height of H and the flow rates of the solvent and the solute are \dot{Q}_1 and \dot{Q}_2 , respectively. Assuming a uniform solvent velocity U and $\dot{Q}_1 \gg \dot{Q}_2$, the dimensionless concentration in cylindrical coordinates (θ , $r^* = r/R$) is

$$c^*(r^*, \theta) = \frac{K_0(Pe r^*/4)/Pe}{K_1(Pe/4) - K_0(Pe/4) \cos \theta} \times \{\exp[Pe(r^* - 1)/4]\}^{\cos \theta}, \quad (5)$$

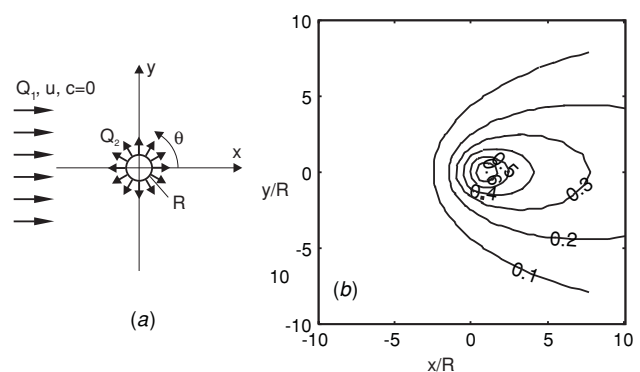


Figure 5. Injection mixer: (a) two-dimensional model and (b) typical dimensionless concentration distribution of a microplume ($Pe = 1$).

where K_0 and K_1 are the modified Bessel functions of the second kind. The Peclet number and the dimensionless concentration are defined as

$$Pe = 2UR/D$$

and

$$c^* = \frac{c}{2\dot{Q}_2/(\pi H)},$$

respectively [56].

Miyake *et al* [51, 52] reported an injection micromixer with 400 nozzles arranged in a square array. The nozzle array is located in a mixing chamber, which is fabricated from silicon using DRIE. Larsen *et al* [53] reported a similar concept with a different nozzle shape. Seidel *et al* [54] and Voldman *et al* [55] utilized capillary forces for generating microplumes. The mixers use a passive valve for releasing one of the two mixed fluids. Table 3 compares the above injection micromixers.

Table 2. Serial lamination micromixers.

Reference	First author	Year	Number of stages	Channel width (μm)	Channel height (μm)	Typical velocity (mm s^{-1})	Re	Pe	Materials
[45]	Branebjerg	1996	3	300	30	1–22	0.03–0.66	15–330	Silicon–glass
[46]	Schwesinger	1996	5–20	400	400	1.8	0.072	72	Silicon–glass
[47]	Gray	1999	6	200	100	n/r	n/r	n/r	Silicon–glass
[48]	Munson	2004	6	600	100	0.5	0.05	50	Mylar
[49]	He	2001	1	100	10	0.25	0.0025	25	Quartz
[50]	Melin	2004	16	50	50	2	0.1	14	Silicon–PDMS

n/r: not reported.

Table 3. Injection micromixers.

Reference	First author	Year	Number of nozzles	Channel width (μm)	Nozzle size (μm)	Channel height (μm)	Typical velocity (mm s^{-1})	Re	Pe	Materials
[51, 52]	Miyake	1993	400	2000	330	15×15	1.2	0.018	18	Silicon–glass
[53]	Larsen	1999	10–20	n/r	$\varnothing 100$	50	1	0.1	100	Silicon–glass
[54]	Seidel	1999	1	280–600	135–175	20–43	n/r	n/r	n/r	Silicon–glass
[55]	Voldman	2000	1	820	7	70	15	0.1	105	Silicon–glass

n/r: not reported.

2.4. Micromixers based on chaotic advection

Besides diffusion, advection is another important form of mass transfer in flows with a low Reynolds number. However, advection is often parallel to the main flow direction, and is not useful for the transversal mixing process. The so-called chaotic advection can improve mixing significantly. Generally, chaotic advection can be generated by special geometries in the mixing channel or induced by an external force. While the first type is a passive micromixer, the second type belongs to the active category and will be discussed later in section 3.

The design concept of micromixers based on chaotic advection is similar to their macroscopic counterparts, which are well investigated and summarized in Ottino's book [17]. The basic idea is the modification of the channel shape for splitting, stretching, folding and breaking of the flow. In the following, micromixers for different ranges of Reynolds number are discussed individually. Although there is no fixed range for a particular design, this review considers the ranges $Re > 100$ as high, $10 < Re < 100$ as intermediate and $Re < 10$ as low.

2.4.1. Chaotic advection at high Reynolds number. The simplest method to get chaotic advection is to insert obstacles structures in the mixing channel. Wang *et al* reported a numerical investigation of obstacles at high Reynolds numbers [57]. The simulated mixing channel is $300 \mu\text{m}$ in width, $100 \mu\text{m}$ in depth and $1.2\text{--}2 \text{ mm}$ in length, and the diameter of the obstacle is $60 \mu\text{m}$ (figure 6(b)). Many arrangements of obstacles were investigated. The simulation assumed a Peclet number of 200. This work found that obstacles in a microchannel at low Reynolds numbers cannot generate eddies or recirculations. However, the results demonstrated that obstacles could improve mixing performance at high Reynolds numbers. Under this condition, the asymmetric arrangement

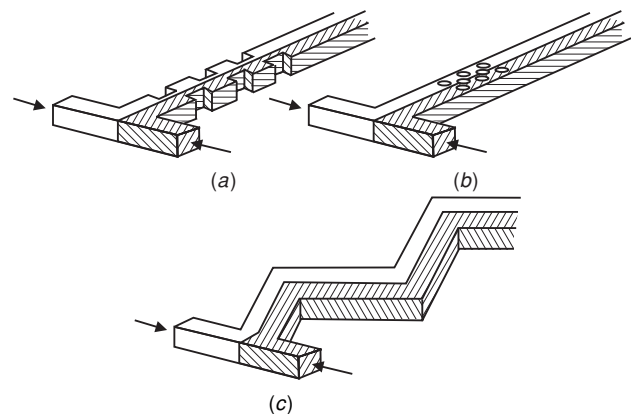


Figure 6. Planar designs for mixing with chaotic advection at high Reynolds numbers: (a) obstacles on wall [30], (b) obstacles in the channel [72, 58] and (c) a zig-zag-shaped channel [59].

of obstacles could alter the flow directions and forces fluids to merge and create transversal mass transport. Lin *et al* [58] used cylinders placed in a narrow channel to enhance mixing. The $50 \mu\text{m} \times 100 \mu\text{m} \times 100 \mu\text{m}$ mixing chamber was fabricated using standard silicon technologies. Seven cylinders of $10 \mu\text{m}$ diameter were arranged in the mixing chamber. The micromixer worked with Reynolds numbers ranging from 200 to 2000 and a mixing time of $50 \mu\text{s}$.

The next method to generate chaotic advection is using zig-zag microchannels to produce recirculation around the turns at high Reynolds numbers. Based on a numerical investigation, Meneaud *et al* [59] discussed the periodic steps of the zig-zag shape as the optimization parameter (figure 6(c)). The micromixers were fabricated using an excimer laser on poly ethylene terephthalate (PET) substrate. The microchannel had a width of $100 \mu\text{m}$, a depth of $48 \mu\text{m}$ and a length of 2 mm . In the simulation, the Peclet number was fixed at 2600 and the Reynolds number ranged from

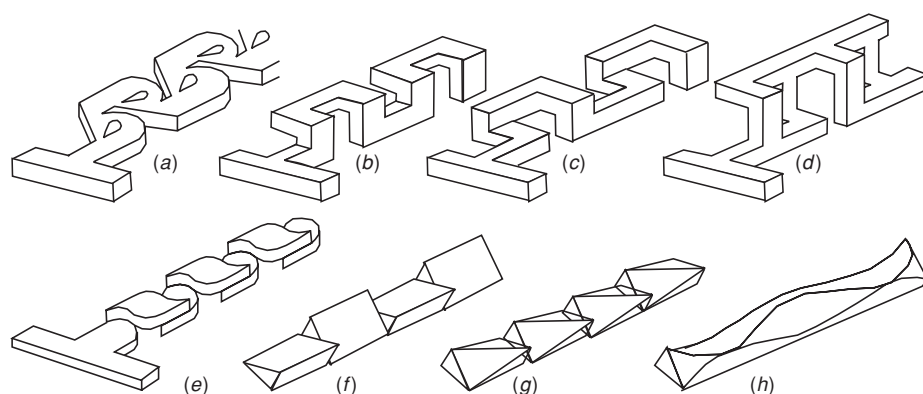


Figure 7. Micromixer designs for mixing with chaotic advection at intermediate Reynolds numbers: (a) modified Tesla structure, (b) C-shape [61], (c) L-shape [62], (d) connected out-of-plane L-shapes [63], (e) twisted microchannel [64] and ((f), (g), (h)) other designs of twisted channel [66].

0.26 to 267. A critical Reynolds number of 80 was observed. Below this number the mixing process relied entirely on molecular diffusion. At higher Reynolds numbers, mixing was improved by the generated recirculations at the turns.

2.4.2. Chaotic advection at intermediate Reynolds numbers.

As mentioned above, micromixers based on chaotic advection can be derived from the macroscale designs with three-dimensionally twisted conduits. However, Hong *et al* [60] demonstrated an inplane micromixer with two-dimensional-modified Tesla structures (figure 7(a)). The Coanda effect in this structure causes chaotic advection and improves mixing significantly. The mixer was made of cyclic olefin copolymer (COC) by hot embossing and thermal direct bonding. The mixer works well at higher Reynolds numbers ($Re > 5$). Liu *et al* [61] reported a three-dimensional serpentine mixing channel fabricated in silicon and glass. The channel was constructed as a series of C-shaped segments positioned in perpendicular planes (figure 7(b)). The micromixer consists of two inlet channels joined in a T-junction, a 7.5 mm long straight channel and a sequence of six mixing segments. The total mixing length was about 20 mm. An interesting observation of the micromixer is that the mixing process is faster at a higher Reynolds number. It shows that chaotic advection only occurs at relatively high Reynolds numbers ($Re = 25\text{--}70$).

Vijayendran *et al* [62] reported a three-dimensional serpentine mixing channel fabricated in PDMS. The channel was designed as a series of L-shaped segments in perpendicular planes (figure 7(c)). The channel has a width of 1 mm and a depth of 300 μm . The total length of the mixing channel is about 30 mm. The mixer was tested at Reynolds numbers of 1, 5 and 20. The experimental results also indicated that better mixing was achieved at higher Reynolds numbers.

Another complex design on PDMS was reported by Chen and Meiners [63]. The mixing unit, called by the authors ‘flow-folding topological structure’, was formed by two connected out-of-plane L-shapes (figure 7(d)). This micromixer was also fabricated in PDMS. The microchannel has a width of 100 μm and a depth of 70 μm . A single mixing unit measures about 400 $\mu\text{m} \times 300 \mu\text{m}$. With this design, effective mixing can be achieved on short length scales with a purely laminar flow ($Re = 0.1\text{--}2$).

Park *et al* reported a more complex three-dimensional micromixer [64]. This work fully utilized the theory on chaotic

advection in Ottino’s book [17] to improve mixing on the microscale with a complex and fine three-dimensional channel shape. The channel rotates and separates the two fluids by partitioning walls and generates smaller blobs exponentially (figure 7(e)). This structure was fabricated with PDMS on glass. Jen *et al* proposed other designs of twisted microchannel in [66]. These designs were not verified by fabricated prototypes. The channel has a width and height of 500 μm and 300 μm , respectively. Mixing of methanol and oxygen at different velocities (0.5 m s^{-1} to 2.5 m s^{-1}) was considered in the simulation (figures 7(f)–(h)).

A planar pulsed source–sink system can also cause chaotic advection in a mixing chamber [67]. The mixer was fabricated in silicon on a 1 cm^2 area. The mixing chamber measures 1500 $\mu\text{m} \times 600 \mu\text{m}$ with a height of 100 μm . For details on this operation principle, readers can refer to [68].

2.4.3. Chaotic advection at low Reynolds numbers.

Similar to macroscale mixers, rips (figure 8(a)) or grooves (figures 8(b) and (c)) on the channel wall can produce chaotic advection. Johnson *et al* [69] were the first to investigate this phenomena. In their work, the grooves were ablated on the bottom wall using a laser. This structure allows an electrokinetic flow to mix at a relatively slow velocity of 300 $\mu\text{m s}^{-1}$. These micromixers were fabricated by excimer laser ablation on a polycarbonate sheet (PC) covered with poly ethylene terephthalate glycol (PETG). The mixing channel was 72 μm wide at the top, 28 μm wide at the bottom and 31 μm deep. The width of an ablated groove was 14 μm and the centre-to-centre spacing between the grooves was 35 μm . The length of the region occupied by the wells from the T-junction was 178 μm .

Almost at the same time, Stroock *et al* investigated this effect and published their results in *Science* [70]. Two different groove patterns were considered (figures 8(b) and (c)). The so-called staggered herringbone mixer (figure 8(b)) can work well at a Reynolds number range from 1 to 100. This concept can be applied to electrokinetic flow by modifying the surface charge [71]. The effect of chaotic advection with the ripped channel was numerically investigated by Wang *et al* [72]. The length, width and depth of the channels were 5 mm, 200 μm and 100 μm , respectively. The mean velocity ranged from 100 $\mu\text{m s}^{-1}$ to 50 mm s^{-1} . The grooves were also ablated on

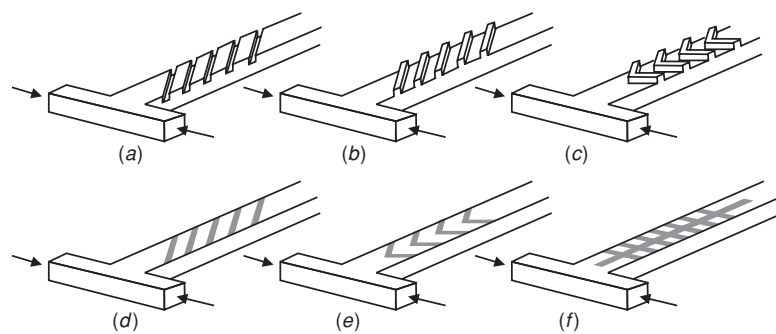


Figure 8. Modification of mixing channel for chaotic advection at low Reynolds numbers: (a) slanted ribs, (b) slanted grooves [70, 71], (c) staggered-herringbone grooves [70, 71] and (d)–(f) patterns for surface modification in a micromixer with electrokinetic flows [74].

the PDMS substrate by a laser [73]. Electrokinetic mixing [74] with only a patterned surface modification can also enhance mixing (figures 8(d) and (f)). With a field strength of $70\text{--}555\text{ V cm}^{-1}$ along the 1.8 mm long microchannel, Biddiss *et al* reported an improvement of mixing efficiencies by 22–68% at Peclet numbers ranging from 190 to 1500. The concept of surface modification can be found in the paper of Hau *et al* [75].

Kim *et al* [76] improved the design of Stroock *et al* [70] with embedded barriers parallel to the flow direction. The mixing channel of this design is $240\text{ }\mu\text{m}$ in width, $60\text{ }\mu\text{m}$ in depth and 21 mm in length. The barriers have a cross section of $40\text{ }\mu\text{m} \times 30\text{ }\mu\text{m}$. This embedded barrier changes the original elliptic mixing pattern [70] to a hyperbolic pattern [76].

A miniaturized version of a conventional mixer with helical elements was reported by Bertsch *et al* [77]. This conventional static mixer with helical elements is also called the Kenics static mixer [78]. The concept changed the three-dimensional inner surface of a cylindrical mixing channel. Two designs were reported for this mixer type. The first design was formed by four mixing elements, which were made of 24 rectangular bars placed at 45° . The four mixing elements were arranged at 45° in the channel. The second design consists of right-handed and left-handed helical elements containing six small-helix structures. The micromixer was fabricated by stereo microphotography, which builds up the complex structure layer by layer. Table 4 summarizes the most important parameters of the above chaotic advection micromixers.

2.5. Droplet micromixers

Another solution for reducing the mixing path is to form droplets of the mixed liquids. The movement of a droplet causes an internal flow field and makes mixing inside the droplet possible. In general, droplets can be generated and transported individually using pressure [79] or capillary effects such as thermocapillary [80] and electrowetting [81]. Furthermore, droplets can be generated due to the large difference of surface forces in a small channel with multiple immiscible phases such as oil/water or water/gas [82].

Hosokawa *et al* [79] reported the earliest droplet micromixer, which was fabricated in PDMS and covered by a PMMA sheet. The concept utilized a hydrophobic microcapillary vent, which joined the two initial droplets.

By simplifying the mass transport equation and introducing an effective dispersion coefficient for a rectangular channel, Handique and Burns reported an analytical model for droplet mixing actuated by thermocapillary [80].

The droplet micromixer can also be transported by electrowetting. Paik *et al* [81] reported different mixing schemes with the electrowetting concept. Droplets can be merged and split repeatedly to generate the mixing pattern. The merged droplet can then be transported around using electrowetting.

The other droplet micromixer design used flow instability between two immiscible liquids [82, 83]. Using a carrier liquid such as oil, droplets of the aqueous samples are formed. While moving through the microchannel, the shear force between the carrier liquid and the sample accelerated the mixing process in the droplet. Table 5 lists some parameters of the above droplet mixers.

3. Active micromixers

3.1. Pressure field disturbance

Pressure field disturbance was used in one of the earliest active micromixers. Deshmukh *et al* [84] reported a T-mixer with pressure disturbance (figure 9(a)). The mixer is integrated in a microfluidic system, which is fabricated in silicon using DRIE. An integrated planar micropump drives and stops the flow in the mixing channel to divide the mixed liquids into serial segments and make the mixing process independent of convection (figure 9(a)). The performance of this micromixer was later discussed by Deshmukh *et al* in their other paper [85]. The pressure disturbance can also be generated by an external micropump [86].

Another alternative method to pressure disturbance is the generation of pulsing velocity [87, 88] (figure 9(b)). Glasgow and Aubry [87] demonstrated a simple T-mixer and its simulation with a pulsed side flow at a small Reynolds number of 0.3. The paper did not elaborate further on the generation of the pulsed flow. In the work of Niu and Lee [88], the pressure disturbance was achieved by introducing a computer controlled source–sink system. This design is partly similar to that of Evans *et al* [67]. The performance of the mixing process is related to the pulse frequency and the number of mixing units. A further modelling work on pressure disturbance was reported by Okkels and Tabeling

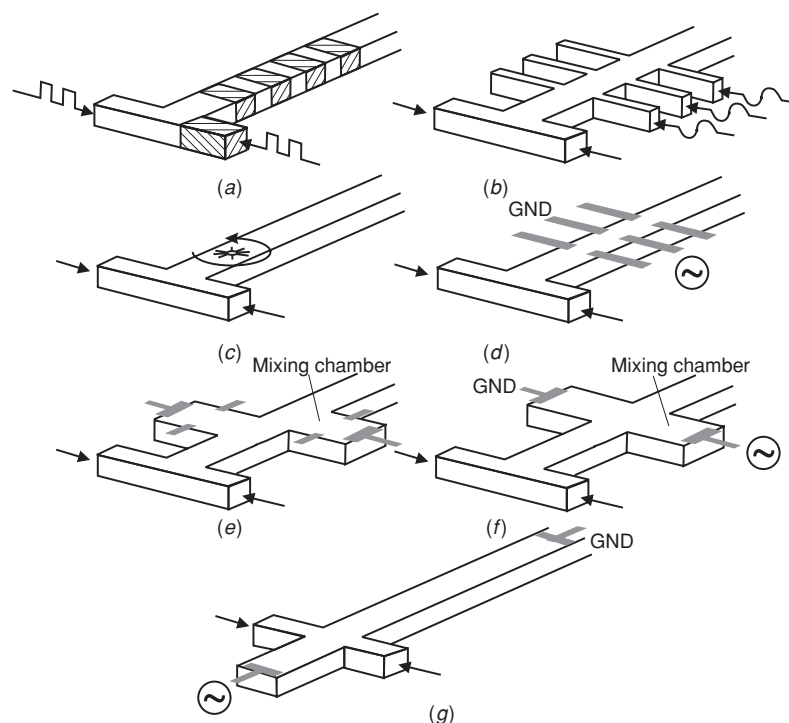


Figure 9. Active micromixers: (a) serial segmentation, (b) pressure disturbance along the mixing channel, (c) integrated microstirrer in the mixing channel, (d) electrohydrodynamic disturbance, (e) dielectrophoretic disturbance, (f) electrokinetic disturbance in the mixing chamber and (g) electrokinetic disturbance in the mixing channel.

Table 4. Chaotic advection micromixers.

Reference	First author	Year	Type	Channel width (μm)	Channel height (μm)	Typical velocity (mm s^{-1})	Re	Pe	Materials
[57]	Wang	2002	Cylindrical obstacles	300	100	0.17	0.25	51	n/a
[58]	Lin	2003	Cylindrical obstacles	10	100	20	0.2	200	Silicon-glass
[59]	Mengeaud	2002	Zig-zag shaped	100	48	1.3–40	0.26–267	130–4000	Mylar
[60]	Hong	2004	2D Tesla	200	90	5	6.2	10^4	COC
[61]	Liu	2000	3D serpentine	300	150	30–350	6–70	$9000\text{--}10^4$	Silicon-glass
[62]	Vijayendran	2003	3D serpentine	1000	300	2–40	1–20	$2000\text{--}(4 \times 10^4)$	PDMS
[63]	Chen	2004	3D serpentine	100	70	1–20	0.1–2	10–200	PDMS
[64]	Park	2004	3D serpentine	100	50	n/r	1–50	0.015–0.7	PDMS
[66]	Jen	2003	3D serpentine	500	300	2000	48	0.36	n/a
[67]	Evans	1997	Source-sink	1500×600	100	n/r	n/r	n/r	Silicon-glass
[69]	Johnson	2002	Patterned wall	72	31	0.6	0.024	15	PC-PETG
[70, 71]	Stroock	2002	Patterned wall	200	70	15	0.01	3000	PDMS
[72]	Wang	2003	Patterned wall	200	100	0.1–50	0.0013–6.65	$20\text{--}10^4$	PDMS
[74]	Biddiss	2004	Patterned wall	200	8	0.01–0.09	0.08–0.7	190–1500	PDMS
[76]	Kim	2004	Patterned wall	240	60	11.6	0.5	2784	PDMS

n/r: not reported; n/a: not applicable.

Table 5. Droplet micromixers.

Reference	First author	Year	Transport type	Droplet size (nl)	Channel width (μm)	Channel height (μm)	Materials
[79]	Hosokawa	1999	Pressure driven	10	100	150	PDMS/PMMA
[81]	Paik	2003	Electrowetting	1600	2480	600–1000	Glass
[82]	Song	2003	Multiple phases	75–150	20–100	n/r	PDMS

n/r: not reported.

[89]. However, the analysis focused only on the mixing pattern in the chamber.

Suzuki and Ho [90] reported a micromixer with integrated conductors. The electrical conductors generate a magnetic field, which in turn moves magnetic beads of 1–10 μm in diameter. The disturbance caused by the magnetic beads improves mixing significantly. Disturbance can also be generated by an integrated magnetic microstirrer as reported by Lu *et al* [91] (figure 9(c)). The micromachined stirrer is placed at the interface between two liquids in a T-mixer. An external magnetic field drives the stirrer at a speed between 100 rpm and 600 rpm.

3.2. Electrohydrodynamic disturbance

The structure of the micromixer with electrohydrodynamic disturbance [92] is similar to the concept reported by Niu and Lee [88]. Instead of pressure sources, electrodes are placed along the mixing channel (figure 9(d)). The mixing channel is 30 mm long, 250 μm wide and 250 μm deep. A series of titanium wires is placed in the direction perpendicular to the mixing channel. By changing the voltage and frequency on the electrodes good mixing was achieved after less than 0.1 s at a low Reynolds number of 0.02.

3.3. Dielectrophoretic disturbance

Dielectrophoresis (DEP) is the polarization of a particle relatively to its surrounding medium in a non-uniform electrical field. This effect causes the particle to move to and from an electrode. Deval *et al* [93] and Lee *et al* [94] reported a dielectrophoretic micromixer. Chaotic advection was generated by embedded particles with a combination of electrical actuation and local geometry channel variation (figure 9(e)).

3.4. Electrokinetic disturbance

As mentioned above, electrokinetic flow can be used to transport liquid in micromixers as an alternative to pressure-driven flow. Jacobson *et al* [41] reported electrokinetically driven mixing in a conventional T-mixer. Lettieri *et al* proposed the use of the electrokinetic effect to disturb the pressure-driven flow in a micromixer [95]. In another case [96], oscillating electro-osmotic flow in a mixing chamber is caused by an ac voltage. The pressure-driven flow becomes instable in a mixing chamber (figure 9(f)) or in a mixing channel (figure 9(g)).

Tang *et al* also utilized an electrokinetic flow to improve mixing [97]. Similar to the previous pressure-driven approach [84], switching on or off the voltage supplied to the flow generates fluid segments in the mixing channel. This flow modulation scheme was capable of injecting reproducible and stable fluid segments into microchannels at a frequency between 0.01 Hz and 1 Hz.

3.5. Magneto hydrodynamic disturbance

The magneto hydrodynamic effect [98] has been used in micromixers. In the presence of an external magnetic field applied dc voltages on the electrodes generate Lorentz forces, which in turn induces mixing movement in the chamber. The

Lorentz force can roll and fold the liquids in a mixing chamber. This concept only works with an electrolyte solution. The mixer of Bau *et al* [98] was fabricated from co-fired ceramic tapes. The electrodes are printed with a gold paste.

3.6. Acoustic disturbance

Acoustic actuators were used to stir fluids in micromixers. The proof of concept for acoustic mixing was reported by Moroney *et al* [99] with a flexible-plate-wave (FPW) device. Zhu and Kim [100] gave an analysis of the focused acoustic wave model in a mixing chamber. They demonstrated an acoustic micromixer fabricated in silicon. The mixing chamber measures 1 mm \times 1 mm \times 10 μm . A zinc oxide membrane is located at the bottom of the mixing chamber. The vibration can be controlled by changing the frequency and the voltage of the input signal. The concept of acoustically induced flow, or acoustic streaming, was also used as an active mixing scheme [101]. Focused acoustic streaming with different electrode patterns was used for mixing [102]. Besides the integrated design, stirring at high frequency can also be realized by an external pump [103].

Ultrasonic mixing may have problems in applications for biological and chemical analysis. The reason is the temperature rise caused by acoustic energy. Many biological fluids are highly sensitive to temperature. Furthermore, ultrasonic waves around 50 kHz are harmful to biological samples because of the possible cavitations. The acoustic micromixer reported by Yasuda [104] used loosely focused acoustic waves to generate stirring movements. The wave was generated by a piezoelectric zinc oxide thin film. The actuator was driven by a sinusoidal wave with frequencies corresponding to the thickness-mode resonance (e.g., 240 MHz and 480 MHz) of the piezoelectric film. The mixer operated without any significant temperature increase and could be used for temperature-sensitive fluids. Further acoustic devices for mixing water and ethanol as well as water and uranine were reported by Yang *et al* [105, 106].

Liu *et al* [107, 108] used acoustic streaming induced around an air bubble for mixing. In this mixer, air pockets with a 500 μm diameter and 500 μm in depth were used for trapping air bubbles. Acoustic streaming was induced by the field generated by an integrated PZT actuator. Yaralioglu *et al* [109] also utilized acoustic streaming to disturb the flow in a conventional Y-mixer. While the channel was made of PDMS, the acoustic actuator was integrated into the cover quartz wafer. A 8 μm thick zinc oxide layer with gold electrodes works as the actuator.

3.7. Thermal disturbance

Since the diffusion coefficient depends highly on temperature, thermal energy can also be used to enhance mixing [110, 111]. Mao *et al* [110] generated a linear temperature gradient across a number of parallel channels in order to investigate the temperature dependence of fluorescent dyes. This approach can possibly be used for micromixing. The other design [111] utilized a thermal bubble to generate disturbance in a mixing channel. Table 6 compares the above active micromixers.

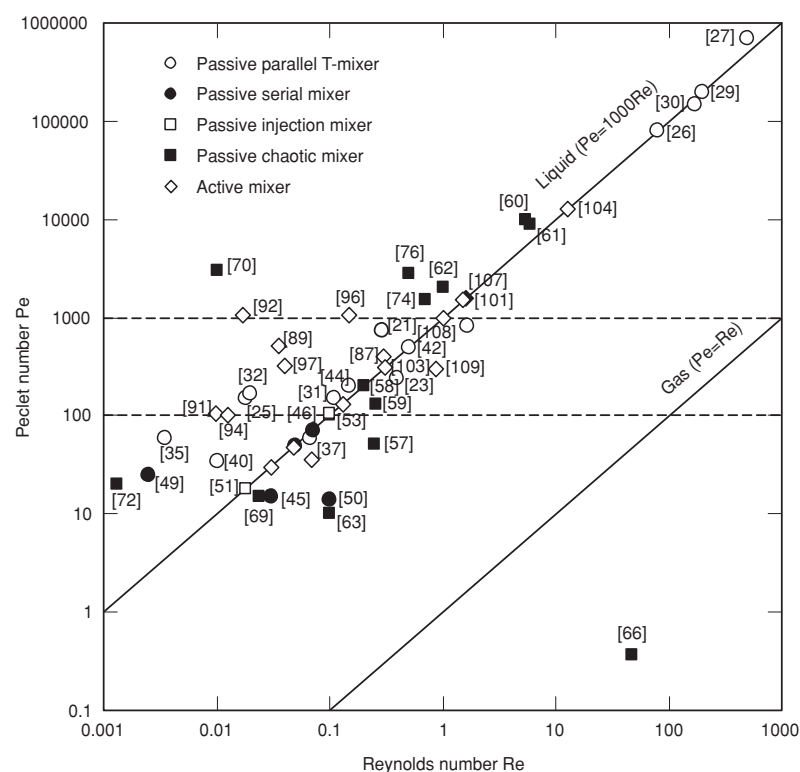


Figure 10. Typical operation ranges of micromixers. The Reynolds number represents the flow range in the mixing channel, while the Peclet number represents the ratio between convection and diffusion. The common flow range in microfluidic devices is $Re < 1$. The data points were determined based on reported geometry data and velocity (flow rate) data. If the kinematic viscosity ν and the diffusion coefficient D are unknown, characteristic values for liquids of $\nu = 1 \times 10^{-6} \text{ m}^2 \text{ s}^{-1}$ and $D = 1 \times 10^{-9} \text{ m}^2 \text{ s}^{-1}$ are assumed. The two characteristic lines $Pe = 1000 Re$ and $Pe = Re$ for liquids and gases, respectively, are explained in the text.

Table 6. Active micromixers.

Reference	First author	Year	Disturbance	Channel width (μm)	Channel height (μm)	Typical velocity (mm s^{-1})	Frequency (Hz)	Re	Pe	St	Materials
[85]	Deshmukh	2001	Pressure	400	78	0.09	1	0.01	36	4.4	Silicon-glass
[86]	Fuji	2003	Pressure	150	150	0.9	100	0.13	133	17	PDMS
[87]	Glasgow	2003	Pressure	200	120	2	0.3	0.3	400	0.03	n/a
[89]	Okkels	2004	Pressure	200	26	1.6	0.85	0.04	321	0.11	PDMS
[90]	Suzuki	2002	Pressure	160	35	0.3	0.02	0.05	48	4	Silicon-glass
[91]	Lu	2002	Pressure	750	70	0.14	5	0.01	105	n/a	PDMS-glass
[92]	El Moutar	2003	Electrohydrodynamic	250	250	4.2	0.5	0.02	1050	0.03	n/a
[93]	Deval	2002	Dielectrophoretic	50	25	0.5	1	0.02	25	0.1	Si-SU8-glass
[94]	Lee	2001	Electrokinetic	200	25	0.5	1	0.01	100	0.4	n/a
[96]	Oddy	2001	Electrokinetic	1000	300	0.5	10	0.15	1050	20	PDMS-glass
[97]	Tang	2002	Electrokinetic	500	35	1	0.17	0.04	509	0.09	PDMS-glass
[98]	Bau	2001	Magneto hydrodynamic	4700	1000	n/r	n/r	n/r	n/r	n/r	Ceramic
[99]	Moroney	1991	Acoustic	1000	400	0.5	10	0.15	1050	20	Si-glass
[101]	Rife	2000	Acoustic	1600	1600	1	n/r	1.6	1600	n/r	n/r
[104]	Yasuda	2000	Acoustic	2000	2000	6.4	n/r	12.8	12 800	n/r	Si-glass
[106]	Yang	2001	Acoustic	6000	60	0.5	n/r	0.03	30	n/r	Si-glass
[107]	Liu	2002	Acoustic	15 000	300	5	n/r	1.5	1500	n/r	Si-glass
[109]	Yaralioglu	2004	Acoustic	300	50	1	n/r	0.86	300	n/r	PDMS-quartz

n/r: not reported; n/a: not applicable.

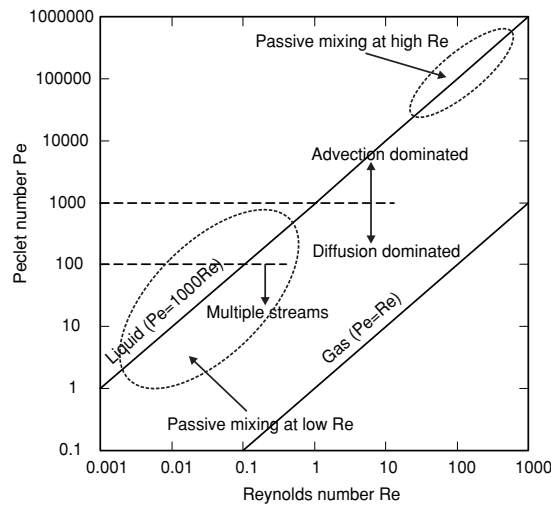


Figure 11. The $Pe-Re$ diagram. Passive micromixers either work at low Reynolds numbers and low Peclet numbers (bottom left corner) or at high Reynolds numbers in the transition regime to turbulence (top right corner). Operation points of passive mixers based on chaotic advection and active mixers can be distributed around the characteristic lines for liquids and gases for a wide range of Reynolds numbers. Passive lamination micromixers with multiple streams have typically small Peclet numbers ($Pe < 100$). In the range of ($Pe < 1000$), the mixer can be considered as diffusion based.

4. Discussions

4.1. Operation conditions

The operation conditions of micromixers can be determined by the characteristic dimensionless numbers such as the Reynolds number Re and Peclet number Pe . From the definitions (1) and (2), the relation between Pe and Re can be derived as

$$\frac{Pe}{Re} = \frac{L}{D_h} \frac{\nu}{D}. \quad (6)$$

The hydraulic diameter D_h and the mixing path L are usually on the same order, therefore we can assume $L/D_h \approx 1$. The kinematic viscosity and the diffusion coefficient of liquids are on the order $\nu = 10^{-6} \text{ m}^2 \text{ s}^{-1}$ and $D = 10^{-9} \text{ m}^2 \text{ s}^{-1}$, respectively. Thus, based on (6) the relation between the Peclet number and Reynolds number can be estimated for liquids as $Pe \approx 1000 Re$. On a $Pr-Re$ diagram, the relation $Pe = 1000 Re$ represents a straight line. Operation points of micromixers for liquids are expected to be around this line. Similarly, for gases with a typical kinematic viscosity and a diffusion coefficients of $\nu = 10^{-5} \text{ m}^2 \text{ s}^{-1}$ and $D = 10^{-5} \text{ m}^2 \text{ s}^{-1}$, the operation point can be expected around the line of $Pe = Re$. Figure 10 depicts the operation points of the mixers reviewed in this paper with the two characteristic lines for gases and liquids. The Reynolds and Peclet numbers are calculated based on the typical values of kinematic viscosity and diffusion coefficient mentioned above, if no further data are given in the particular work.

The data points in figure 10 show the clear two operation areas for liquids and gases. Many points are lying above the $Pe = 1000 Re$ line, because the ratio between the mixing path L and the hydraulic diameter D_h is more than unity in most cases. In a planar microfluidic system the channel width,

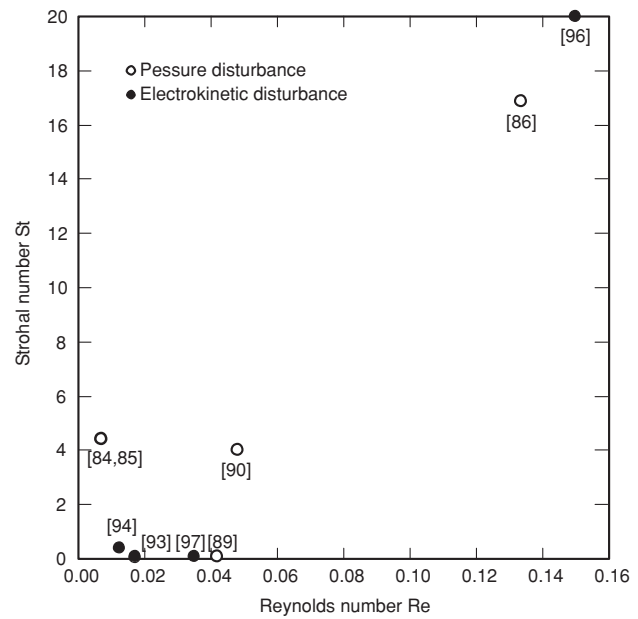


Figure 12. The $St-Re$ diagram. The Strohal number represents the ratio between residence time and the time period of the disturbance. The data indicate that a higher Reynolds number (high flow velocity) requires a larger Strohal number (a higher disturbance frequency).

which usually represents the mixing path, is much larger than the channel height, which is usually close to the value of the hydraulic diameter. Figure 11 depicts the most important characteristics of a $Pe-Re$ diagram.

Figure 12 depicts the typical Strohal numbers of active micromixers with pressure disturbance and electrokinetic disturbance. We can clearly observe that a higher Reynolds number requires a higher Strohal number. A fast flow has a short residence time in the mixing channel, thus a shorter time period or a higher disturbance frequency is needed for full mixing. Since the disturbance frequency depends on the dynamics of the external actuator, the Reynolds number or the flow rate of the mixer should be designed to match a given disturbance frequency.

4.2. Fabrication methods

A variety of fabrication techniques have been used for making micromixers. The different techniques can be categorized as silicon micromachining and polymeric micromachining.

Most of the early micromixers were made of silicon. The mixing channels were either wet etched with KOH [21, 35, 45, 46, 51, 61] or dry etched using deep reactive ion etching (DRIE) [27, 29, 32, 37, 47, 55, 58, 84]. A glass cover is anodically bonded on top of the channel offering both sealing and optical access. Passive micromixers can be made entirely of glass [39–41]. In some applications such as mixing of electrokinetic flows, silicon cannot be used because of its electrically conducting properties. Most active micromixers with integrated actuators are fabricated in silicon because of established technologies [90, 99, 103, 106] such as sputtering of metals and piezoelectric materials.

Besides the advantages of an established technology, silicon-based micromixers are relatively expensive because of the large surface needed for microchannels and the

required clean room facilities. Furthermore, silicon devices are not always chemically and biochemically compatible. Polymeric micromachining offers a lower fabrication cost and a faster prototyping cycle. A simple approach established by Whitesides's group [112] at Harvard University has been repeated recently by many other groups [28, 44, 70, 71, 96, 97]. This low-cost approach uses a lithography mask printed from a high-resolution laser printer. The mask is then used for the subsequent photolithography of the thick-film negative resist SU-8 on a silicon wafer. The SU-8/silicon wafer works as a mold for an elastomer such as polydimethylsiloxane (PDMS). After a surface treatment in oxygen plasma, the PDMS part with the microchannels can be covered by a glass plate, which provides both optical transparency and mechanical rigidity for the device. Several PDMS layers can be fabricated in the same way and bonded directly to form a complex three-dimensional structure [62–64, 76]. For direct bonding, methanol was used for self-alignment between the PDMS layers. Because of its sealing property, PDMS can also be used as the adhesion layer between glass and silicon [42].

The thick-film resist SU-8 can be used directly for making micromixers. SU-8 microchannels were formed on a silicon or glass substrate [33, 93]. SU-8 has the advantage of simple micromachining. Moveable structures such as microvalves [113] and microgrippers [114] have been fabricated with the so-called polymeric surface micromachining. This approach proves the feasibility of making a complex microfluidic system with moveable structures in SU-8.

Mixing channels were also fabricated by hot embossing with a hard template, which can be micromachined in silicon [69], glass, or metals such as nickel [60]. This approach is limited to a two-dimensional channel structure but promises a simple method for mass production. Fast prototyping can be achieved with laser micromachining of thin polymer and adhesive sheets [25, 48]. However, the resolution of this approach is limited by the wavelength of the laser.

4.3. Characterization techniques

Despite the numerous recent works on micromixers, characterization of micromixers still remains a challenge. The quantification of the extent of mixing is important for evaluation of performance as well as design optimization of micromixers.

The common quantification technique is using dilution of a tracer dye to determine the extent of mixing. For a low-noise measurement, fluorescent dye and a corresponding microscope with a filter set is required. The intensity image can then be recorded and evaluated. Since the concentration of the dye is proportional to the intensity of the recorded image, the uniformity of the concentration image can be quantified by determining the standard deviation of the pixel intensity values [61, 70]. In some cases, if the standard deviation of intensity values cannot resolve the differences between regions in the image, spatial probability density functions (PDF) of intensities integrated over finite regions can be used to quantify mixing [96]. Furthermore, the two-dimensional power spectrum of the intensity image can also be considered as another quantification method [96, 88].

The above techniques are statistical methods, which depend on the orientation of the mixed fluids relative to the

imaging direction. If the imaging direction is perpendicular to the fluid layers as in the case of the mixer reported by Hinsmann *et al* [24], the two layers, even at the channel entrance, appear to be completely mixed. In such cases, an imaging system with a confocal microscope is required for the three-dimensional spatial distribution of the concentration field [23, 42].

Another quantification method is measuring the fluorescent product of a chemical reaction [21]. The intensity of the product is a direct measure of the extent of mixing. Typically, this process is an acid–base reaction with a dye having a fluorescence quantum yield that is pH dependent. Recently, Munson and Yager [48] reported a new concept for the quantification of mixing. The method relies on the increase of intensity of fluorescein at basic pH. In this method, both liquids are diluted with fluorescein. They only have different buffers with different pH values. The increase in fluorescence in the initially acidic solution overwhelms the small decrease in fluorescence of the other solution. The total fluorescence increases by a factor of 2 and can work as a measure for the extent of mixing [48].

4.4. Applications of micromixers

Micromixers are widely used in chemical, biological and medical analysis fields. Almost every chemical assay requires mixing of reagents with a sample.

The basic T-mixer was used in the work of Kamholz *et al* [21] for the measurement of analyte concentrations of a continuous flow. The concentration of a target analyte is measured by the fluorescence intensity of the region where the analyte and a fluorescent indicator have interdiffused [21, 23]. The micromixer reported by Hinsmann *et al* [24] was used for the study of rapid chemical reactions in solution with stopped-flow time resolved Fourier transform infrared spectroscopy (TR-FTIR). Wu *et al* [25] used a Y-mixer for investigating the nonlinear diffusive behaviour of a fluorescein. Micromixers can be used as sensors in environmental monitoring such as the detection of ammonia in aqueous solutions [32]. The fast mixing time in a micromixer benefits time-resolved measurement of reaction kinetics using nuclear magnetic resonance (NMR) [38]. Fluri *et al* [39] combines capillary electrophoresis (CE) separation with a T-mixer as a postcolumn reactor. An electrokinetically driven T-mixer was used in [40] for performing enzyme assays. The short mixing length of a cross-mixer with hydrodynamic focusing makes the fast infection of a cell with a virus possible [44]. Fast mixing with a micromixer was used in the freeze–quenching technique, which is useful for trapping meta-stable intermediates populated during fast chemical or biochemical reactions [58]. In [62], micromixers were used for the sample preparation of a surface-based biosensor.

Besides sensing and analysis applications as discussed above, micromixers were used as a tool for dispersing immiscible liquids and forming micro droplets [36]. Furthermore, micromixers work as a separator for particles based on their different diffusion coefficients [115, 116] or as a generator of concentration gradients [118–122].

5. Summary

The development of micromixers has been progressing rapidly in recent years. From the early devices made of silicon and glass, a number of polymeric micromixers have been fabricated and successfully tested. Due to their simple designs, passive micromixers found the most applications in analytical chemistry. While conventional parallel lamination mixers work well at low Reynolds numbers and low Peclet numbers, micromixers based on chaotic advection can be designed to suit a wide range of Reynolds numbers. Mixing with chaotic advection does not depend on the Peclet number. This review paper discussed the different designs of micromixers and their operation conditions. With a trend for polymeric microfluidic systems, a simple but efficient passive micromixer is the choice for many applications in chemical and biochemical analyses.

References

- [1] Nguyen N T and Wereley S T 2002 *Fundamentals and Applications of Microfluidics* (Boston: Artech House)
- [2] Oosterbroek R E and van den Berg A 2003 *Lab-on-a-Chip: Miniaturized System for Bio(Chemical) Analysis and Synthesis* (Amsterdam: Elsevier)
- [3] Geschke O, Klank H and Tellemann P 2004 *Microsystem Engineering of Lab-on-a-Chip Devices* 2nd edn (New York: Wiley)
- [4] Nguyen N T, Huang X Y and Toh K C 2002 MEMS—micropumps: a review *ASME Trans.—J. Fluids Eng.* **124** 384–92
- [5] Laser D J and Santiago J G 2004 A review of micropumps *J. Micromech. Microeng.* **11** R35–64
- [6] Woias P 2004 Micropumps—past, progress and future prospects *Sensors Actuators B* at press
- [7] Kakuta M, Bessoth F G and Manz A 2001 Microfabricated devices for fluid mixing and their application for chemical synthesis *Chem. Rec.* **1** 395–405
- [8] Reyes D R *et al* 2002 Micro total analysis systems: 1. Introduction, theory, and technology *Anal. Chem.* **74** 2623–36
- [9] Auroux P A *et al* 2002 Micro total analysis systems: 2. Analytical standard operations and applications *Anal. Chem.* **74** 2637–52
- [10] Vilkner T *et al* 2004 Micro total analysis systems. Recent developments *Anal. Chem.* **76** 3373–86
- [11] Erbacher C *et al* 1999 Towards integrated continuous-flow chemical reactors *Mikrochim. Acta* **131** 19–24
- [12] Madou M J 2002 *Fundamentals of Microfabrication: The Science of Miniaturization* 2nd edn (Boca Raton: CRC Press)
- [13] Einstein A 1956 *Investigations on the Theory of the Brownian Movements* (New York: Dover)
- [14] Ottino J M 1990 Mixing, chaotic advection, and turbulence *Annu. Rev. Fluid Mech.* **22** 207–53
- [15] Brodsky R S 1975 *Turbulence in Mixing Operations* (New York: Academic)
- [16] Ottino J M 1989 The mixing of fluids *Sci. Am.* **January** 55–67
- [17] Ottino J M 1989 *The Kinematics of Mixing: Stretching, Chaos, and Transport* (Cambridge, New York: Cambridge University Press)
- [18] Cussler E L 1984 *Diffusion Mass Transfer in Fluid Systems* (New York: Cambridge University Press)
- [19] Cunningham R E and William R J J 1980 *Diffusion in Gases and Porous Media* (New York: Plenum)
- [20] Bird R B *et al* 2002 *Transport Phenomena* (New York: Wiley)
- [21] Kamholz A E *et al* 1999 Quantitative analysis of molecular interactive in microfluidic channel: the T-sensor *Anal. Chem.* **71** 5340–7
- [22] Kamholz A E and Yager P 2002 Molecular diffusive scaling laws in pressure-driven microfluidic channels: deviation from one-dimensional Einstein approximations *Sensor Actuators B* **82** 117–21
- [23] Ismagilov R F *et al* 2000 Experimental and theoretical scaling laws for transverse diffusive broadening in two-phase laminar flows in microchannels *Appl. Phys. Lett.* **76** 2376–78
- [24] Hinsmann P *et al* 2001 Design, simulation and application of a new micromixing device for time resolved infrared spectroscopy of chemical reactions in solutions *Lab on a Chip* **1** 16–21
- [25] Wu Z, Nguyen N T and Huang X Y 2004 Non-linear diffusive mixing in microchannels: theory and experiments *J. Micromech. Microeng.* **14** 604–11
- [26] Yi M and Bau H H 2003 The kinematics of bend-induced mixing in micro-conduits *Int. J. Heat Fluid Flow* **24** 645–56
- [27] Wong S H, Ward M C L and Wharton C W 2004 Micro T-mixer as a rapid mixing micromixer *Sensors Actuators B* **100** 365–85
- [28] Lim D S W *et al* 2003 Dynamic formation of ring-shaped patterns of colloidal particles in microfluidic systems *Appl. Phys. Lett.* **83** 1145–7
- [29] Böhm S *et al* A rapid vortex micromixer for studying high-speed chemical reactions *Technical Proc. Micro Total Analysis Systems MicroTAS 2001 (Monterey, CA, USA)* 25–7
- [30] Wong S H *et al* 2003 Investigation of mixing in a cross-shaped micromixer with static mixing elements for reaction kinetics studies *Sensors Actuators B* **95** 414–24
- [31] Gobby D, Angeli P and Gavrilidis A 2001 Mixing characteristics of T-type microfluidic mixers *J. Micromech. Microeng.* **11** 126–32
- [32] Veenstra T T 1999 Characterization method for a new diffusion mixer applicable in micro flow injection analysis systems *J. Micromech. Microeng.* **9** 199–202
- [33] Jackman R J *et al* 2001 Microfluidic systems with on-line UV detection fabricated in photodefineable epoxy *J. Micromech. Microeng.* **11** 263–9
- [34] Möbius *et al* 1995 A sensor controlled process in chemical microreactors *Proc. Transducers '95, 8th Int. Conf. on Solid-State Sensors and Actuators (Stockholm, Sweden)* pp 775–8
- [35] Koch M *et al* 1999 Improved characterization technique for micromixers *J. Micromech. Microeng.* **9** 156–8
- [36] Haverkamp V *et al* 1999 The potential of micromixers for contacting of disperse liquid phases *Fresenius' J. Anal. Chem.* **364** 617–24
- [37] Bessoth F G, de Mello A J and Manz A 1999 Microstructure for efficient continuous flow mixing *Anal. Commun.* **36** 213–5
- [38] Kakuta M *et al* 2003 Micromixer-based time-resolved NMR: applications to ubiquitin protein conformation *Anal. Chem.* **75** 956–60
- [39] Fluri K *et al* 1996 Integrated capillary electrophoresis devices with an efficient postcolumn reactor in planar quartz and glass chips *Anal. Chem.* **68** 4285–90
- [40] Hadd A G *et al* 1997 Microchip device for performing enzyme assays *Anal. Chem.* **69** 3407–12
- [41] Jacobson S C, McKnight T E and Ramsey J M 1999 Microfluidic devices for electrokinetically driven parallel and serial mixing *Anal. Chem.* **71** 4455–9
- [42] Knight J B, Vishwanath A, Brody J P and Austin R H 1998 Hydrodynamic focusing on a silicon chip: mixing nanoliters in microseconds *Phys. Rev. Lett.* **80** 3863–6
- [43] Jensen K 1998 Chemical kinetics: smaller, faster chemistry *Nature* **393** 735–6

- [44] Walker G M, Ozers M S and Beebe D J 2004 Cell infection within a microfluidic device using virus gradients *Sensors Actuators B* **98** 347–55
- [45] Branebjerg J *et al* 1996 Fast mixing by lamination *Proc. MEMS'96, 9th IEEE Int. Workshop Micro Electromechanical System (San Diego, CA)* pp 441–6
- [46] Schwesinger N *et al* 1996 A modular microfluid system with an integrated micromixer *J. Micromech. Microeng.* **6** 99–102
- [47] Gray B L *et al* 1999 Novel interconnection technologies for integrated microfluidic systems *Sensors Actuators A* **77** 57–65
- [48] Munson M S and Yager P 2004 Simple quantitative optical method for monitoring the extent of mixing applied to a novel microfluidic mixer *Anal. Chim. Acta* **507** 63–71
- [49] He B *et al* 2001 A picoliter–volume mixer for microfluidic analytical systems *Anal. Chem.* **73** 1942–7
- [50] Melin J *et al* 2004 A fast passive and planar liquid sample micromixer *Lab on a Chip* **4** at press
- [51] Miyake R *et al* 1993 Micro mixer with fast diffusion *Proc. MEMS'93, 6th IEEE Int. Workshop Micro Electromechanical System (San Diego, CA)* pp 248–53
- [52] Miyake R *et al* 1997 A highly sensitive and small flow-type chemical analysis system with integrated absorptionmetric micro-flowcell *Proc. MEMS'97, 10th IEEE Int. Workshop Micro Electromechanical System (Nagoya, Japan)* pp 102–7
- [53] Larsen U D, Rong W and Telleman P 1999 Design of rapid micromixers using CFD *Proc. Transducers'99, 10th Int. Conf. on Solid-State Sensors and Actuators (Sendai, Japan)* pp 200–3
- [54] Seidel R U *et al* 1999 Capillary force mixing device as sampling module for chemical analysis *Proc. Transducers'99, 10th Int. Conf. on Solid-State Sensors and Actuators (Sendai, Japan)* pp 438–41
- [55] Voldman J, Gray M L and Schmidt M A 2000 An integrated liquid mixer/valve *J. Microelectromech. Syst.* **9** 295–302
- [56] Nguyen N T 2004 *Mikrofluidik: Entwurf, Herstellung und Charakterisierung* (Stuttgart: Teubner Verlag)
- [57] Wang H *et al* 2002 Optimizing layout of obstacles for enhanced mixing in microchannels *Smart Mater. Struct.* **11** 662–7
- [58] Lin Y *et al* 2003 Ultrafast microfluidic mixer and freeze–quenching device *Anal. Chem.* **75** 5381–6
- [59] Mengeaud V, Jossierand J and Girault H H 2002 Mixing processes in a zigzag microchannel: finite element simulation and optical study *Anal. Chem.* **74** 4279–86
- [60] Hong C C, Choi J W and Ahn C H 2004 A novel in-plane microfluidic mixer with modified tesla structures *Lab on a Chip* **4** 109–13
- [61] Liu R H *et al* 2000 Passive mixing in a three-dimensional serpentine microchannel *J. Microelectromech. Syst.* **9** 190–7
- [62] Vijayendran *et al* 2003 Evaluation of a three-dimensional micromixer in a surface-based biosensor *Langmuir* **19** 1824–28
- [63] Chen H and Meiners J C 2004 Topologic mixing on a microfluidic chip *Appl. Phys. Lett.* **84** 2193–5
- [64] Park S J *et al* 2004 Rapid three-dimensional passive rotation micromixer using the breakup process *J. Micromech. Microeng.* **14** 6–14
- [65] Mizuno Y and Funakoshi M 2002 Chaotic mixing due to a spatially periodic three-dimensional flow *Fluid Dyn. Res.* **31** 129–49
- [66] Jen C P *et al* 2003 Design and simulation of the micromixer with chaotic advection in twisted microchannels *Lab on a Chip* **3** 77–81
- [67] Evans J, Liepmann D and Pisano A P 1997 Planar laminar mixer *Proc. MEMS'97, 10th IEEE Int. Workshop Micro Electromechanical System (Nagoya, Japan)* pp 96–101
- [68] Johnes S and Aref H 1988 Chaotic advection in pulsed source–sink systems *Phys. Fluids* **31** 469–85
- [69] Johnson T J, Ross D and Locascio L E 2002 Rapid microfluidic mixing *Anal. Chem.* **74** 45–51
- [70] Stroock A D *et al* 2002 Chaotic mixer for microchannels *Science* **295** 647–51
- [71] Stroock A D and Whitesides G M 2003 Controlling flows in microchannels with patterned surface charge and topography *Acc. Chem. Res.* **36** 597–604
- [72] Wang H *et al* 2003 Numerical investigation of mixing in microchannels with patterned grooves *J. Micromech. Microeng.* **13** 801–8
- [73] Lim D *et al* 2003 Fabrication of microfluidic mixers and artificial vasculatures using a high-brightness diode-pumped Nd:YAG laser direct write method *Lab on a Chip* **3** 318–23
- [74] Biddiss E, Erickson D and Li D 2004 Heterogeneous surface charge enhanced micromixing for electrokinetic flows *Anal. Chem.* **76** 3208–13
- [75] Hau W I *et al* 2003 Surface-chemistry technology for microfluidics *J. Micromech. Microeng.* **13** 272–8
- [76] Kim D S *et al* 2004 A barrier embedded chaotic micromixer *J. Micromech. Microeng.* **14** 798–805
- [77] Bertsch A *et al* 2001 Static micromixers based on large-scale industrial mixer geometry *Lab on a Chip* **1** 56–60
- [78] Bertsch A *et al* 1998 Laminar flow in static mixer with helical elements online at <http://www.bakker.org/cfmbook/lamstat.pdf>
- [79] Hosokawa K, Fujii T and Endo I 1999 Droplet-based nano/picoliter mixer using hydrophobic microcapillary vent *Proc. the IEEE International Workshop Micro Electromechanical System (Piscataway, NJ, USA)* pp 388–93
- [80] Handique K and Burns M A 2001 Mathematical modeling of drop mixing in a slit-type microchannel *J. Micromech. Microeng.* **11** 548–54
- [81] Paik P, Pamula V K and Fair R B 2003 Rapid droplet mixers for digital microfluidic systems *Lab on a Chip* **3** 253–9
- [82] Song H *et al* 2003 Experimental test of scaling of mixing by chaotic advection in droplets moving through microfluidic channels *Appl. Phys. Lett.* **83** 4664–6
- [83] Tice J D, Lyon A D and Ismagilov R F 2003 Effects of viscosity on droplet formation and mixing in microfluidic channels *Anal. Chim. Acta* **507** 73–7
- [84] Deshmukh A A, Liepmann D and Pisano A P 2000 Continuous micromixer with pulsatile micropumps *Technical Digest of the IEEE Solid State Sensor and Actuator Workshop (Hilton Head Island, SC)* pp 73–6
- [85] Deshmukh A A, Liepmann D and Pisano A P 2001 Characterization of a micro-mixing, pumping, and valving system *Proc. Transducers'01, 11th Int. Conf. on Solid-State Sensors and Actuators (Munich, Germany)* pp 779–82
- [86] Fujii *et al* 2003 A plug and play microfluidic device *Lab on a Chip* **3** 193–7
- [87] Glasgow I and Aubry N 2003 Enhancement of microfluidic mixing using time pulsing *Lab on a Chip* **3** 114–20
- [88] Niu X Z and Lee Y K 2003 Efficient spatial–temporal chaotic mixing in microchannels *J. Micromech. Microeng.* **13** 454–62
- [89] Okkels F and Tabeling P 2004 Spatiotemporal resonances in mixing of open viscous fluids *Phys. Rev. Lett.* **92** 038301
- [90] Suzuki H and Ho C M 2002 A magnetic force driven chaotic micro-mixer *Proc. MEMS'02, 15th IEEE Int. Workshop Micro Electromechanical System (Las Vegas, Nevada)* pp 40–3
- [91] Lu L H, Ryu K S and Liu C 2002 A magnetic microstirrer and array for microfluidic mixing *J. Microelectromech. Syst.* **11** 462–9
- [92] El Mactar A O, Aubry N and Batton J 2003 Electro–hydrodynamic micro–fluidic mixer *Lab on a Chip* **3** 273–80
- [93] Deval J, Tabeling P and Ho C M 2002 A dielectrophoretic chaotic mixer *Proc. MEMS'02, 15th IEEE Int. Workshop*

- Micro Electromechanical System (Las Vegas, Nevada)* pp 36–9
- [94] Lee Y K *et al* 2001 Chaotic mixing in electrokinetically and pressure driven micro flows *Proc. MEMS'01, 14th IEEE Int. Workshop Micro Electromechanical System (Interlaken, Switzerland)* pp 483–6
- [95] Lettieri G L *et al* 2000 Consequences of opposing electrokinetically and pressure-induced flows in microchannels of varying geometries *Proc. Micro Total Analysis Systems (Enschede, NL)* pp 351–4
- [96] Oddy M H, Santiago J G and Mikkelsen J C 2001 Electrokinetic instability micromixing *Anal. Chem.* **73** 5822–32
- [97] Tang Z *et al* 2002 Electrokinetic flow control for composition modulation in a microchannel *J. Micromech. Microeng.* **12** 870–7
- [98] Bau H H, Zhong J and Yi M 2001 A minute magneto hydro dynamic (MHD) mixer *Sensors Actuators B* **79** 207–15
- [99] Moroney R M, White R M and Howe R T 1991 Ultrasonically induced microtransport *Proc. MEMS'91, 3th IEEE Int. Workshop Micro Electromechanical System (Nara, Japan)* pp 277–82
- [100] Zhu X and Kim E S 1997 Acoustic-wave liquid mixer *Microelectromechanical Systems (MEMS) American Society of Mechanical Engineers, Dynamic Systems and Control Division (Publication) DSC vol 62 (ASME, Fairfield, NJ, USA)* pp 35–8
- [101] Rife J C *et al* 2000 Miniature valveless ultrasonic pumps and mixers *Sensors Actuators A* **86** 135–40
- [102] Vivek V, Zeng Y and Kim E S 2000 Novel acoustic-wave micromixer *Proc. MEMS'00, 13th IEEE Int. Workshop Micro Electromechanical System (Miyazaki, Japan)* pp 668–73
- [103] Woias P, Hauser K and Yacoub-George E 2000 An active silicon micromixer for mTAS applications *Micro Total Analysis Systems 2000 (Boston, MA)* pp 277–82
- [104] Yasuda K 2000 Non-destructive, non-contact handling method for biomaterials in micro-chamber by ultrasound *Sensors Actuators B* **64** 128–35
- [105] Yang Z *et al* 2000 Active micromixer for microfluidic systems using lead-zirconate-titanate (PZT)-generated ultrasonic vibration *Electrophoresis* **21** 116–9
- [106] Yang Z *et al* 2001 Ultrasonic micromixer for microfluidic systems *Sensors Actuators A* **93** 266–72
- [107] Liu R H *et al* 2002 Bubble-induced acoustic micromixing *Lab on a Chip* **2** 151–7
- [108] Liu R H *et al* 2003 Hybridization enhancement using cavitation microstreaming *Anal. Chem.* **75** 1911–7
- [109] Yaralioglu G G *et al* 2004 Ultrasonic mixing in microfluidic channels using integrated transducers *Anal. Chem.* **76** 3694–8
- [110] Mao H, Yang T and Cremer P S 2002 A microfluidic device with a linear temperature gradient for parallel and combinatorial measurements *J. Am. Chem. Soc.* **124** 4432–5
- [111] Tsai J H and Lin L 2002 Active microfluidic mixer and gas bubble filter driven by thermal bubble pump *Sensors Actuators A* **97–98** 665–71
- [112] Duffy D, McDonald J, Schueller O and Whitesides G 1998 Rapid prototyping of microfluidic systems in poly(dimethylsiloxane) *Anal. Chem.* **70** 4974–84
- [113] Nguyen N T *et al* 2003 Micro checkvalves for integration into polymeric microfluidic devices *J. Micromech. Microeng.* **14** 69–75
- [114] Nguyen N T *et al* 2004 A polymeric microgripper with integrated thermal actuators *J. Micromech. Microeng.* **14** 969–74
- [115] Brody J P and Yager P 1997 Diffusion-based extraction in a microfabricated device *Sensors Actuators A* **58** 13–8
- [116] Weigl B and Yager P 1999 Microfluidic diffusion-based separation and detection *Science* **283** 346–7
- [117] Hatch A *et al* 2001 A rapid diffusion immunoassay in a T-sensor *Nat. Biotechnol.* **19** 461–5
- [118] Burke B J and Regnier F E 2003 Stopped-flow enzyme assays on a chip using a microfabricated mixer *Anal. Chem.* **75** 1786–91
- [119] Dertinger S K W *et al* 2001 Generation of gradients having complex shapes using microfluidic networks *Anal. Chem.* **73** 1240–6
- [120] Holden M A *et al* 2003 Generating fixed concentration array in a microfluidic device *Sensors Actuators B* **92** 199–207
- [121] Holden M A *et al* 2003 Microfluidic diffusion diluter: bulging of PDMS microchannels under pressure-driven flow *J. Micromech. Microeng.* **13** 412–8
- [122] Yang M *et al* 2002 Generation of concentration gradient by controlled flow distribution and diffusive mixing in a microfluidic chip *Lab on a Chip* **2** 158–63